

## 4D STEM with an Ultrafast Camera Reveals Mesoscale Structure in Anisotropic Molecular Glass Thin Films

Debaditya Chatterjee<sup>1</sup>, Shuoyuan Huang<sup>1</sup>, Kaichen Gu<sup>2,4</sup>, Junguang Yu<sup>3</sup>, Harald Bock<sup>5</sup>, Lian Yu<sup>3</sup>, Mark Ediger<sup>2</sup>, and Paul M. Voyles<sup>1\*</sup>

<sup>1</sup> Department of Materials Science and Engineering, University of Wisconsin-Madison, Madison, WI 53706, USA

<sup>2</sup> Department of Chemistry, University of Wisconsin-Madison, Madison, WI 53706, USA

<sup>3</sup> School of Pharmacy, University of Wisconsin-Madison, Madison, WI 53705, USA

<sup>4</sup> Exponent, New Territories, Hong Kong SAR, China

<sup>5</sup> Centre de Recherche Paul Pascal – Centre national de la recherche scientifique, 33600 Pessac, France

\* Corresponding author: paul.voyles@wisc.edu

Glassy thin films of organic semiconductors prepared by physical vapor deposition (PVD) can exhibit an unusual form of structure: the molecules have a preferred orientation without long-range translational symmetry. We have used low-dose four dimensional scanning transmission electron microscopy (4D STEM) enabled by a fast direct electron detector to map the domain structure that occupies the length scale between the orientation of a single molecule and the global disorder of the glass.

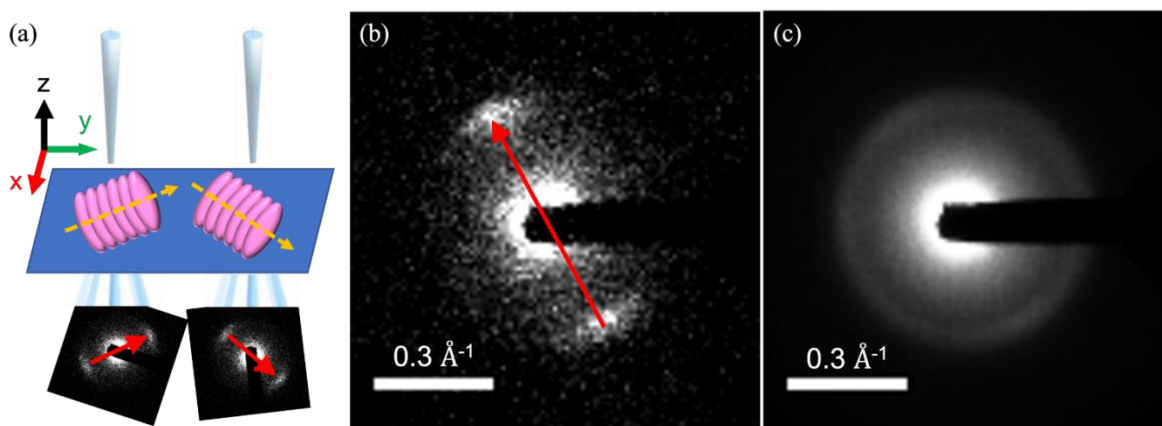
We have studied films of a phenanthroperylene ester, which is a discotic mesogen with an equilibrium columnar hexagonal liquid crystalline phase that favors anisotropic charge and exciton transport [1], and order that can be tuned over a wide range of length scales [2]. Physical vapor deposition allows us to make glasses that have high thermal stability and tunable structural anisotropy arising from a surface equilibration mechanism during deposition [3]. Intracolumnar charge transport along the  $\pi$ - $\pi$  stacking direction is much more efficient than intercolumnar transport, so the length scale of  $\pi$ - $\pi$  stacked columns strongly impacts the charge-transport mobility in electronic devices [1, 4]. Measuring the persistence length of columnar orientation and the nature of column connectivity across the plane of these PVD films and understanding the mechanism of growth of ordered domains during deposition is essential to developing materials for optoelectronic devices.

Figure 1(a) shows a schematic of the 4D STEM experiment. Illuminating regions on the sample with varying columnar order lets us capture diffraction patterns with Bragg peaks oriented in different directions. Figure 1(b) shows a representative diffraction pattern from a single columnar orientation. The red arrow highlights the local column orientation. The spacing between the discotic molecules is  $\sim 3.5$  Å leading to diffraction arcs at  $\sim 0.286$  Å<sup>-1</sup>. Figure 1(c) shows the averaged diffraction pattern across all probe positions on a sample. The uniform ring indicates a lack of any long-range preferred orientation. Processing many diffraction patterns acquired from a grid of probe positions creates a map of the local orientation. Similar experiments have been performed previously on semicrystalline polymers [5, 6], but the phenanthroperylene ester films are less structurally ordered and more beam-sensitive. (We find that they sustain only  $\sim 100$  e<sup>-</sup>/Å<sup>2</sup> at 200 kV before losing orientational order.) Studying this material at low dose is made possible by a new, ultrafast direct electron detection camera [7] operated at 0.125 ms per diffraction pattern for these experiments, and a 0.1 nm step size between probe positions, with a 0.6 pA, 2 nm diameter probe. The resulting 4D STEM datasets can be several TBs, so analysis required significant extensions to data analysis libraries like pyXEM and Hyperspy [8].

Figure 2 shows column orientation maps from samples processed at different conditions, revealing variations in the length scale of ordering. The glass transition temperature ( $T_g$ ) of this system is 392 K. Figures 2 (a) and (b) are from 40 nm PVD films deposited at 0.25 Å/s at substrate temperatures of 380 K ( $0.97 T_g$ ) and 392 K ( $T_g$ ) respectively. Figure 2 (c) is from a liquid-cooled sample prepared by heating up a PVD film to 457 K into its liquid crystalline phase and cooling to room temperature at 2.5 K/min. The orientation maps show the columnar orientation as an angle between  $0^\circ$  and  $180^\circ$  with respect to horizontal as indicated by the arrows and the color. The colors highlight domains with similar orientations. Figs 2(a) and (b) show that the film grown at a higher substrate temperature has larger domains, and Fig 2(c) shows that the liquid-cooled sample has much larger domains, 100s of nanometers across. The liquid-cooled orientation map also exhibits focal conics, a common liquid crystal defect. These results probe an essential intermediate length scale between the orientation of each molecule previously probed by X-ray diffraction and ellipsometry [2] and the long-range disorder of the film's structure.

The molecular orientation during PVD film growth is anchored by the free surface configuration [3], and the surfaces of these materials are highly mobile. As a result, the domain size is related to the balance between surface residence time and mobility. We measure that the mean domain sizes in the films grown at substrate temperatures of 380 K and 392 K are  $27 \pm 2$  nm and  $45 \pm 3$  nm respectively, yielding a domain size ratio,  $\frac{d(392 K)}{d(380 K)} = 1.7 \pm 0.3$ . Assuming that the surface diffusivity of the molecules during film growth has an Arrhenius temperature dependence with the orientational ordering activation energy of 110 kJ/mol [2] we get  $\sqrt{\frac{D_s(392 K)}{D_s(380 K)}} = 1.70$ . This agreement showing that the domain sizes scale with the square root of the surface diffusivity during deposition, indicates that a diffusion limited growth mechanism controls the size of the domains.

We have shown how low dose 4D STEM with a fast direct electron detector enables the study of mesoscale ordering with nanometer-level spatial resolution in a molecular glass to gain insights into the growth processes during PVD. Future work will focus on growth and characterization of films of molecular glasses with controlled anisotropy [9].



**Figure 1.** (a) 4D STEM experiment schematic. We determine the local columnar orientation using diffraction from the  $\pi$ - $\pi$  stacking of disc shaped molecules. (b) Representative diffraction pattern from a single columnar orientation. The red arrow highlights the local orientation reflected in the diffraction

arcs. (c) Average diffraction pattern from all probe positions across a sample shows a uniform ring.

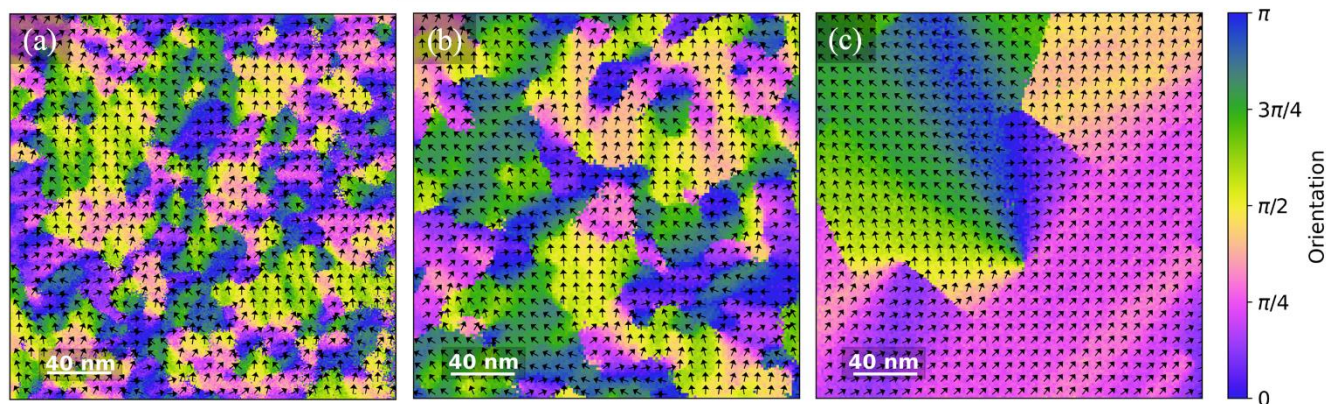


**Figure 2.** Maps of phenanthroperylene ester column orientation in films deposited at 0.25 Å/s. (a) used a substrate temperature of 380 K ( $0.97 T_g$ ), and (b) used 392 K ( $T_g$ ). (c) was heated into its liquid crystalline state at 457 K, then cooled to room temperature at 2.5 K/min. The orientation domain size increases with substrate temperature.

#### References:

- [1] J. Kelber, M.-F. Achard, F. Durola, H. Bock, Distorted Arene Core Allows Room-Temperature Columnar Liquid-Crystal Glass with Minimal Side Chains, *Angew. Chemie Int. Ed.* **51** (2012) 5200–5203. <https://doi.org/10.1002/anie.201108886>.
- [2] C. Bishop, Z. Chen, M.F. Toney, H. Bock, L. Yu, M.D. Ediger, Using Deposition Rate and Substrate Temperature to Manipulate Liquid Crystal-Like Order in a Vapor-Deposited Hexagonal Columnar Glass, *J. Phys. Chem. B.* **125** (2021) 2761–2770. <https://doi.org/10.1021/acs.jpcc.0c11564>.
- [3] K. Bagchi, M.D. Ediger, Controlling Structure and Properties of Vapor-Deposited Glasses of Organic Semiconductors: Recent Advances and Challenges, *J. Phys. Chem. Lett.* **11** (2020) 6935–6945. <https://doi.org/10.1021/acs.jpcclett.0c01682>.
- [4] J. Eccher, W. Zajczkowski, G.C. Faria, H. Bock, H. von Seggern, W. Pisula, I.H. Bechtold, Thermal Evaporation versus Spin-Coating: Electrical Performance in Columnar Liquid Crystal OLEDs, *ACS Appl. Mater. Interfaces.* **7** (2015) 16374–16381. <https://doi.org/10.1021/acsami.5b03496>.
- [5] O. Panova, C. Ophus, C.J. Takacs, K.C. Bustillo, L. Balhorn, A. Salleo, N. Balsara, A.M. Minor, Diffraction imaging of nanocrystalline structures in organic semiconductor molecular thin films, *Nat. Mater.* **18** (2019) 860–865. <https://doi.org/10.1038/s41563-019-0387-3>.
- [6] C. Cendra, L. Balhorn, W. Zhang, K. O'Hara, K. Bruening, C.J. Tassone, H.-G. Steinrück, M. Liang, M.F. Toney, I. McCulloch, M.L. Chabinyk, A. Salleo, C.J. Takacs, Unraveling the Unconventional Order of a High-Mobility Indacenodithiophene–Benzothiadiazole Copolymer, *ACS Macro Lett.* **10** (2021) 1306–1314. <https://doi.org/10.1021/acsmacrolett.1c00547>.
- [7] D. Chatterjee, J. Wei, A. Kvit, B. Bammes, B. Levin, R. Bilhorn, P. Voyles, An Ultrafast Direct Electron Camera for 4D STEM, *Microsc. Microanal.* **27** (2021) 1004–1006. <https://doi.org/10.1017/S1431927621003809>.
- [8] F. De La Peña, et. al., hyperspy/hyperspy: Release v1.6.4, (2021). <https://doi.org/10.5281/zenodo.5082777>.
- [9] The authors gratefully acknowledge support of this research by NSF through the University of Wisconsin Materials Research Science and Engineering Center (DMR-1720415).